

# Microstructure and mechanical properties of macro-defect-free cements

D. BORTZMEYER, L. FROUIN, Y. MONTARDI, G. ORANGE  
*Rhône-Poulenc Recherches, 52 rue de la Haie Coq, Aubervilliers, France*

The mechanical properties of macro-defect-free cements were investigated with the help of fracture mechanics and rheology; transmission electronic microscopy (TEM) and scanning electronic microscopy (SEM) were used to characterize the microstructure. The microstructure was found to consist of nanosized hydration products embedded in a cross-linked polymer matrix. The nanoscale composite structure of the cement is thought to play an important part in the mechanical properties.

## 1. Introduction

Macro-defect-free (MDF) cements described by Birchall *et al.* [1, 2] can be described as cement–polymer composites characterized by very high tensile strengths ( $\sigma_t$  up to 300 MPa). In terms of linear elastic fracture mechanics, these performances are due to both an increase of the critical stress intensity factor,  $K_{IC}$ , and a decrease of the critical defect size,  $a_c$ . Both terms are linked by the well-known Griffith's equation

$$\sigma_t = \frac{K_{IC}}{Y(a_c)^{1/2}} \quad (1)$$

where  $Y$  is a configuration correction factor.

The small critical defect size is a consequence of the MDF process (high shear mixing followed by hot pressing). High  $K_{IC}$  values are usually explained by the ionic cross-linking of the polymer phase lying between the cement grains.

The two main MDF systems described in the literature are calcium aluminate cement–polyvinyl alcohol (CAC–PVA), and calcium silicate cement–polyacrylamid (CSC–PAM). In the CAC–PVA system, cross-linking of PVA hydroxyles by aluminate ions is supposed to occur [3] (Fig. 1), while in the CSC–PAM system, ionic cross-linking between carboxyl groups and calcium ions is invoked [4] (Fig. 2).

The purpose of this work was to provide an insight into the mechanical properties and microstructure of MDF cements.

## 2. Experimental procedure

Both systems (CAC–PVA and CSC–PAM) were studied in order to shed light on the different mechanisms involved in MDF composites. Alumina cement “Secar 71” was used (Lafarge Fondu) with PVA of different molecular weights (Prolabo). The Portland cement, from Ciment de Quentin, was processed with PAM supplied from Aldrich.

The compositions were, in all cases, cement 100 parts (by weight), polymer 7 parts, water 14 parts.

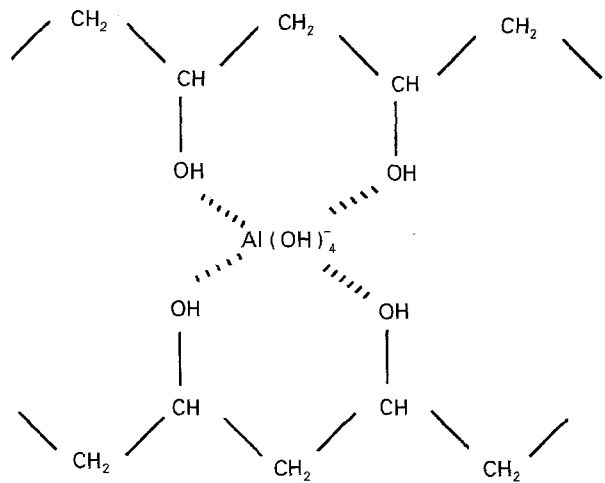


Figure 1 Cross-linking of PVA molecules by aluminate ions.

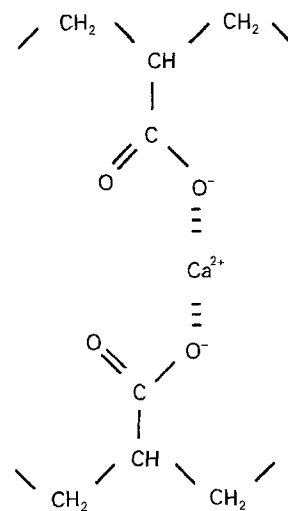


Figure 2 Cross-linking of carboxyl groups by calcium ions.

Glycerol (0.5 parts) was added in the case of CAC–PVA.

The original MDF process consists in calendaring the cement–polymer dough then pressing the sheet at

a rather slight pressure (30 bar) between the platens of a hot press [1, 2]. A slightly different process was used in our case: high shear mixing in a polymer compounder was preferred, followed by hot pressing (80–120 °C) in a closed die (400 bar) for 1 h.

The three-point bending test was used for the measurement of fracture strength, Young's modulus and critical stress intensity factor (notched samples were used for the latter measurement).

SEM examination of fractured surfaces and polished sections was carried out on a Jeol JSM 840 microscope. TEM specimens were prepared by argon-ion milling on a cold stage. Examinations were conducted on a CM30 microscope operated at 300 kV. A liquid-nitrogen-cooled sample holder was proved useful to reduce the degradation of organic and hydrated phases under the electron beam, and to prevent carbon contamination during energy dispersive spectroscopy (EDS) and parallel electron energy loss spectrometry (PEELS) microanalysis.

PVA films cross-linked by aluminate ions were used as a model material, in order to understand the toughening mechanisms of MDF cements. These films were prepared by first dissolving the polymer in the required amount of water (final concentration 150 g l<sup>-1</sup>), then mixing these solutions with the required amount of sodium aluminate ions, and casting the mixture over silicon moulds. The films thickness was about 0.5 mm. Drying was performed at room temperature over 24 h (however, oven-drying did not change the conclusions).

These films were characterized either by dynamic rheology (RDS, Rheometrics) or by direct mechanical testing on rectangular samples.

### 3. Results

#### 3.1. Relationship between microstructure and $K_{IC}$

##### 3.1.1. Influence of polymer molecular weight

Table I compares the properties of our CAC–PVA MDF cements with the properties of a classic cement. Several remarks can be made. The tensile strength of our MDF cements is about 100 MPa, which is lower than the results obtained, for example, by Russell [5] because of the rather low molecular weight, and high water content, used in our case. The critical stress intensity factor of these samples is about 2 MPa m<sup>1/2</sup>, which is a reasonable value for MDF cements [6], while the critical stress intensity factor of classic cements is about 0.3 MPa m<sup>1/2</sup>. The increase in tensile strength is thus due to both an increase of  $K_{IC}$  and a decrease of the critical defect size. Both of these

TABLE I Comparison of a classic cement with our MDF cement (composition as above, PVA 14/135, pressing temperature 100 °C)

	Fracture strength (MPa)	$K_{IC}$ (MPa√m)	$a_c$ (microns)
classic cement	10	0.3	300
MDF cement	110	1.8	48

effects are important. The small critical defect size is a direct consequence of the MDF process (calendering + hot pressing). But the reason for the high  $K_{IC}$  value is not so obvious, and will be discussed below. Polymer cross-linking is often mentioned as the reason for the high critical stress intensity factor of MDF cements. Cross-linking obviously occurs, as has been proved by chemical analysis [4] or dynamical rheology [5].

The mechanical analysis of our CAC–PVA cements proves that the polymer phase plays a major role in the cement properties. The fracture energy has been calculated from the above measurements and is shown in Fig. 3. It is seen that a power law is obtained:  $G_c = \alpha M^n$  with  $n$  about 1/2. In polymer science, the exponent  $n$  is supposed to be equal to 2 due to the reptation mechanism. Depending on the interactions between the polymer chains, exponents from 1/2 to 2 are known to occur [7]. Wasson and Nicholson [8] suggest that an exponent equal to 2 characterizes a classic polymer; ionic interactions between the polymer chains should give about 1; an exponent of 0.5 is proof of a very strong coupling between the polymer chains. So the question is, what sort of cross-linking is that? This will be explored by microstructural analysis and mechanical testing of PVA films.

#### 3.1.2. Analysis of cross-linked PVA films

PVA films containing aluminate ions were cast as described in the experimental section, and tested by dynamic rheology or tensile testing.

The first results were obtained on undried films (they were stored at room temperature and tested 48 h after casting). Fig. 4 shows that the storage modulus of these films increases with the amount of aluminate ions, indicating an increase in cross-linking. The theory of dynamic viscosity of cross-linked polymers [9, 10] states that the storage modulus is linked to the cross-link concentration by

$$G' = \frac{\rho}{M_c} RT \quad (2)$$

where  $\rho$  is the gel density and  $M_c$  the number average molecular weight. Applying Equation 2 to our data indicates that there is about 10<sup>-5</sup> mol l<sup>-1</sup> of cross-link,

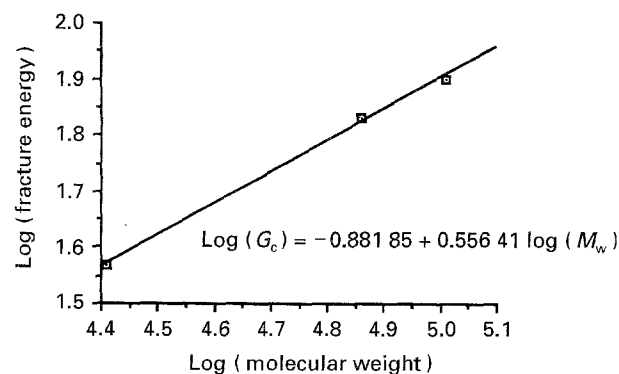


Figure 3 The influence of the molecular weight on the fracture energy in the CAC–PVA system.

i.e. less than 0.1% of the aluminate ions participate in the rigidity of the structure. Such a small amount of "effective" reticulation seems to be normal in such systems [10, 11].

Drying the films (room temperature for a few weeks, or 50 °C for one night) increases their modulus by a factor of 100, but then the modulus of dried films depends only weakly on the aluminate concentration (Fig. 5). Moreover, the tensile strength does not depend on aluminate concentration, for small concentrations. Above a given threshold, an increase in ion concentration causes a decrease of the tensile strength (Fig. 6).

Upon drying, hydrogen interactions between the OH groups of the PVA chains become very strong:

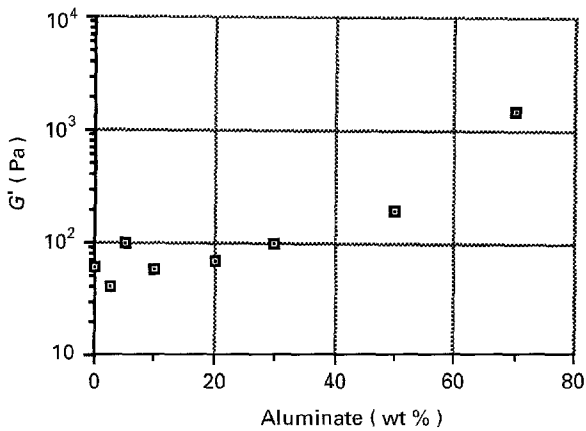


Figure 4 The influence of the aluminate fraction on the storage modulus in PVA–aluminate ion undried films.

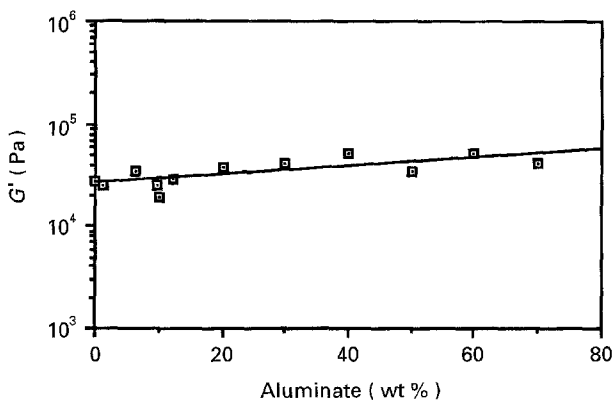


Figure 5 The influence of the aluminate fraction on the storage modulus in PVA–aluminate ion dried films.

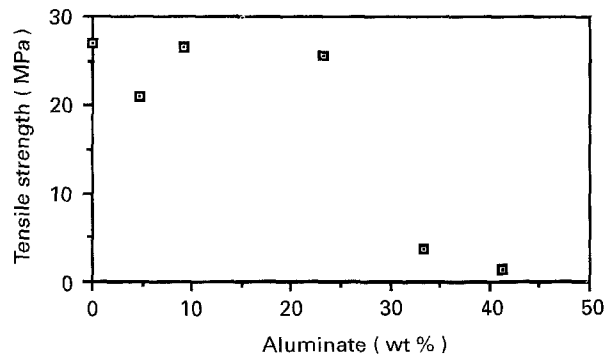


Figure 6 The influence of the aluminate fraction on the tensile strength in PVA–aluminate ion dried films.

this is probably the reason for the very high increase in modulus. As a consequence, the aluminate cross-linking becomes negligible. The tensile strength decrease is due to another phenomenon: while the films without aluminate are translucent, films with aluminate are white, probably because of small sodium aluminate particles. The strength decreases when these particles become too large.

These results prove that in CAC–PVA systems, ionic cross-linking of the polymer is probably not the main direct cause for the high mechanical properties. But obviously, this cross-linking can be an indirect cause (modification of the nature and morphology of the hydrated products). An investigation of the MDF cement microstructure was done in order to examine this problem.

### 3.1.3. Microstructure of MDF cement

The organic matrix surrounding the cement grains is not an homogeneous phase of polymer cross-linked by ions. Popoola *et al.* [3] described it (in the CAC–PVA system) as a carbon-rich phase containing small nano-inclusions of metastable phases.

Our own MDF samples also displayed a very inhomogeneous microstructure. The first interesting microstructural level is the 10 μm scale: Fig. 7, showing a polished surface cut in a Portland–PAM MDF, shows that a large fraction of the cement grains remains non-hydrated. The occurrence of a small crack propagating in the matrix around the grains, shows that the control of the cement packing density is of primary importance for the MDF strength.

The "organic" phase between the cement grains is neither homogeneous (carbon has been detected in this phase through electron energy loss spectrometry (EELS)). Fig. 8 shows a TEM view of this matrix (high resolution electronic microscopy (HREM)), in a CSC–PAM MDF cement. Small inclusions of nanometric crystal are clearly visible. Note that the composition and crystallographic nature of these phases is very difficult to determine. It seems to be very different from one inclusion to another.

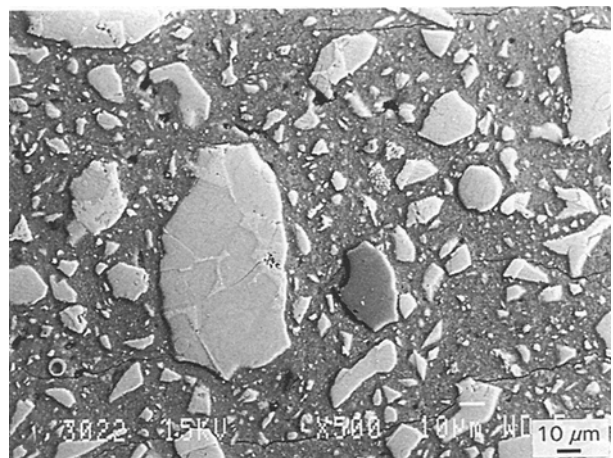
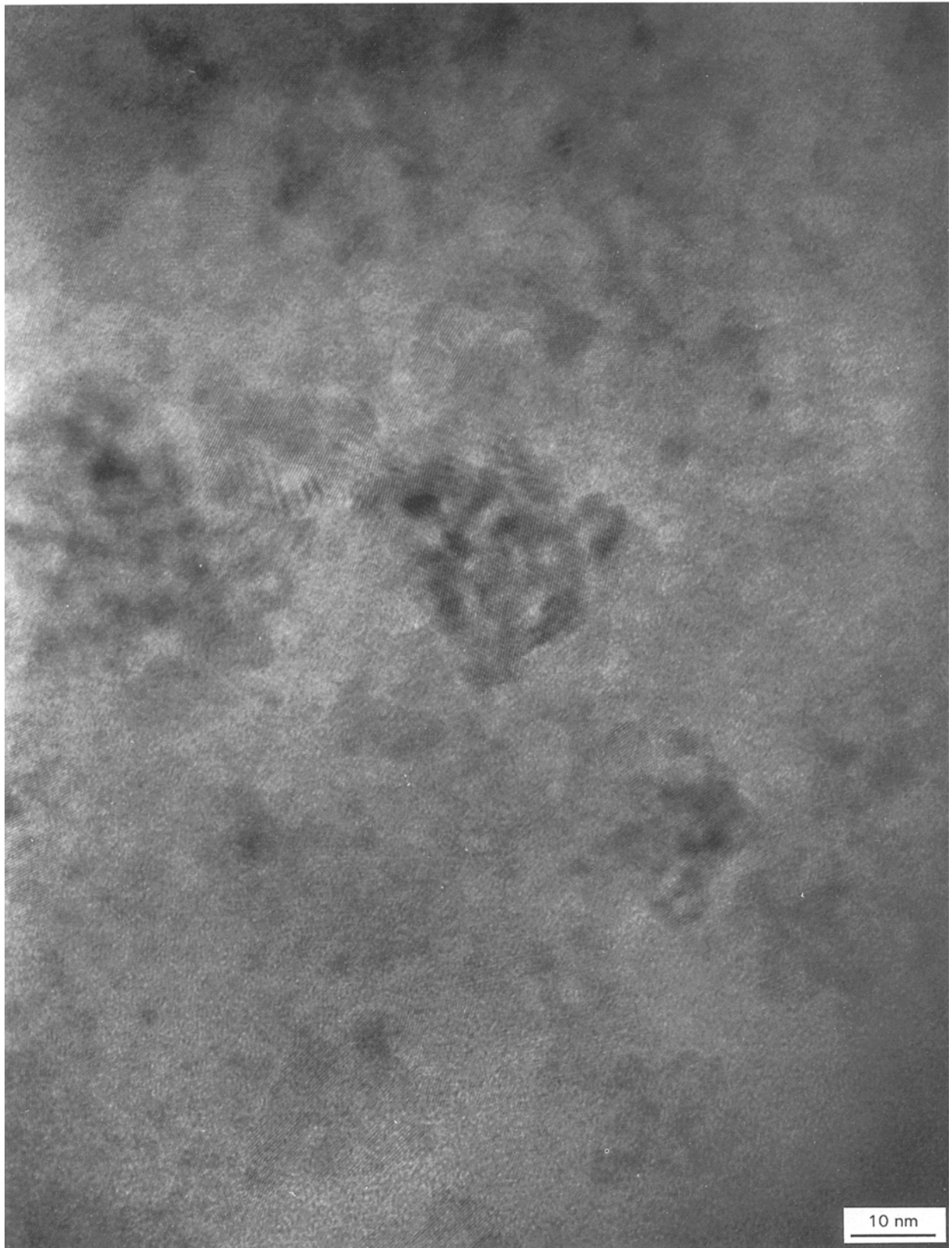


Figure 7 Scanning electron micrograph of a polished surface (back-scattered electron mode) in the CSC–PAM system.



*Figure 8* High-resolution electron micrograph of the “organic” phase, showing inclusions of nanoscale hydrated products in the CSC–PAM system.

These hydrated products have probably nucleated on the hydrophilic sites available on the polymer (anions or cations fixed on the hydroxylic or carboxylic groups). In this way, an important role of the polymer could be to promote the heterogeneous nucleation of hydrated phases and consequently decrease drastically their mean size.

The MDF cement microstructure is thus an example of a “multi-scale” composite: the first scale, 15  $\mu\text{m}$  cement grains in an “organic” phase; this “organic phase”, at a second scale, appears to contain 10–200 nm hydrated nanocrystals embedded in another “organic” phase. This second organic phase consists in polymer chains cross-linked by ions (according

to Popoola *et al.* [3], in the case of the CAC–PVA system, polymer chains may be intercalated between the crystallographic planes of the hydrated products). This composite structure is certainly highly involved in the reinforcing mechanisms which result in the high  $K_{IC}$  values.

The next section will show that the above analysis is not yet sufficient to understand fully the toughening mechanisms of MDF cements.

### 3.1.4. $K_R$ curve of MDF cements

Because of the various mechanisms operating in front of or behind the main propagating crack in non-homogeneous materials, the fracture toughness is often found to increase with crack length (“quasi-brittle materials”) [12, 13]. This is the case in cementitious materials such as concrete, mortar, and cement paste. The constant fracture toughness assumption no longer holds, and the fracture process cannot be adequately described by single fracture parameters such as  $K_{IC}$  or fracture energy  $G_c$ . The concept of a rising crack resistance,  $K_R$ , curve has to be used, allowing an independent determination of the crack initiation and crack propagation steps.

The determination of the rising crack resistance can provide experimental support to explain the toughening and strengthening effects in MDF cements. Different mechanisms may be involved: the formation of a process zone (damaged zone) at the tip of the main crack (shielding effect), crack bridging, and a frictional effect across the newly fractured surfaces (wake effect).

In our experiments, large double-cantilever beams (50 mm × 20 mm × 4 mm) with a pre-crack of 10 mm length were machined from CSC–PAM plates. The specimens were loaded in a closed-loop controlled machine at a low displacement rate, to obtain a stable crack propagation. Using the fracture load and the corresponding crack length, the applied stress intensity factor,  $K$ , and hence the crack resistance,  $K_R$ , can be calculated [14].

Fig. 9 shows the crack resistance curve calculated from experimental values. It is clear that  $K_R$  rises from a low value,  $K_o$ , at about 1.15 MPa m<sup>1/2</sup> to a plateau value  $K_{oo}$  at about 2.18 MPa m<sup>1/2</sup>, over a crack

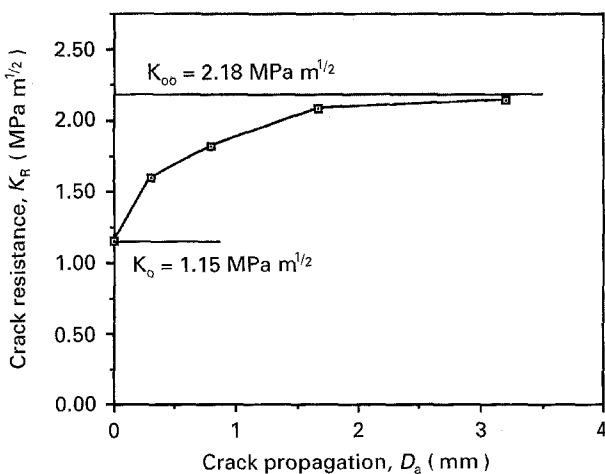


Figure 9  $K_R$  curve for the CSC–PAM system.

growth of approximately 2.5–3 mm. The initiation parameter,  $K_o$ , corresponds to the intrinsic toughness of the material, very close to the crack tip. The plateau value  $K_{oo}$  represents the toughening effect which occurs behind the crack tip, as the main crack propagates.

The high level of toughness observed in MDF cements can thus be attributed to both effects: an increase of the intrinsic toughness of the materials, and the development of a toughening effect as the crack propagates. The increase of intrinsic toughness is probably correlated to the specific microstructure described in the above sections. A wake effect such as bridging is probably operating to explain the toughening as the crack propagates. The microscopic level of the microstructure has to be considered in this case: large cement grains and polymer fibrils.

A crack resistance model based on bridging of crack surfaces has been developed by Mai and Lawn [15]. The effective stress intensity factor at equilibrium is a resultant of a factor due to the applied stress and a counteracting stress intensity factor corresponding to the closure stress. According to this model, the maximum bridging stress,  $\sigma^*$ , at the tip of the crack is calculated to be about 15 MPa.

Thus, the experimental evidence and theoretical analysis of the crack resistance data show that the mechanical properties of MDF cements, and especially the fracture work, are a consequence of both the improved intrinsic toughness and the bridging fracture work.

### 3.2. Influence of processing parameters

The above results gave an insight into the origin of the high critical stress intensity factor of MDF cements. However, as was stated before, the high tensile stress is also due to the low critical defect size. It is interesting to study the influence of the processing parameters on this variable.

As a first example, let us consider the influence of the molecular weight,  $M_w$ , on the mechanical properties in the CAC–PVA system. As was shown in Fig. 3, fracture energy is roughly proportional to  $M_w^{1/2}$ . But, on the other hand, due to an increase in the viscosity

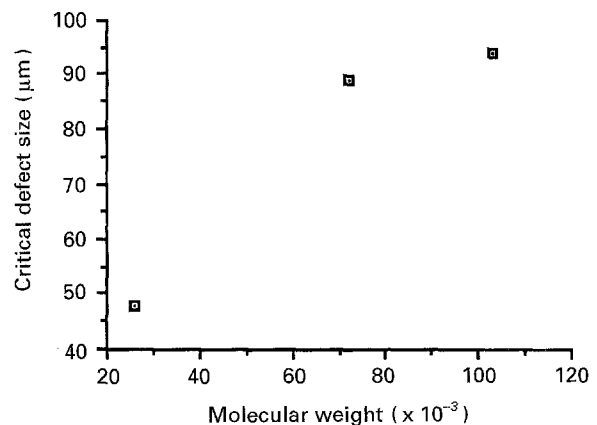


Figure 10 The influence of the molecular weight on the critical defect size in the CAC–PVA system.

of the paste, the critical defect size also increases with  $M_w$  (Fig. 10). As a consequence (Equation 1), the tensile strength shows an optimum (Fig. 11).

In the CSC-PAM system, the pressing temperature has a similar influence. Increasing the pressing temperature increases the critical stress intensity factor (Fig. 12). However, it also increases the critical defect

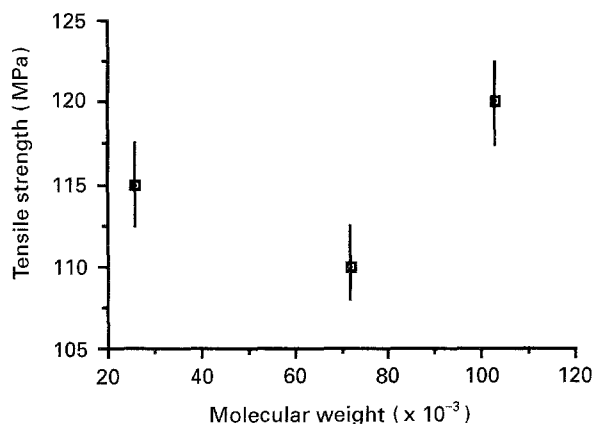


Figure 11 The influence of the molecular weight on the tensile strength in the CAC-PVA system.

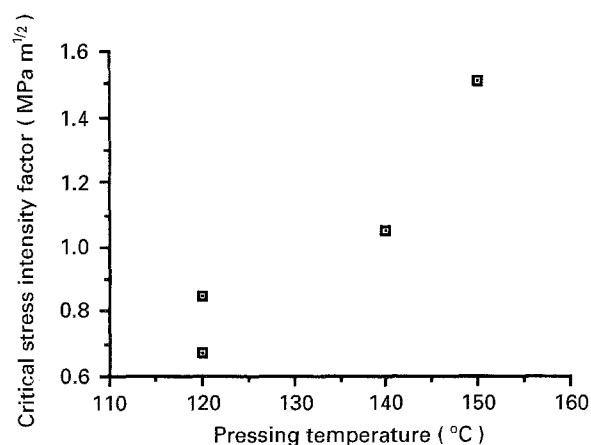


Figure 12 The influence of the pressing temperature on the critical stress intensity factor in the CSC-PAM system.

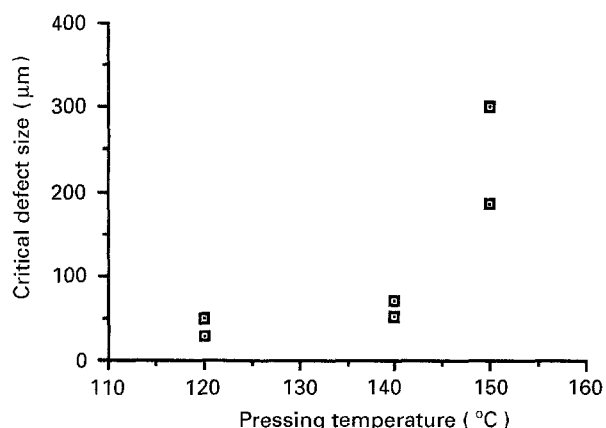


Figure 13 The influence of the pressing temperature on the critical defect size in the CSC-PAM system.

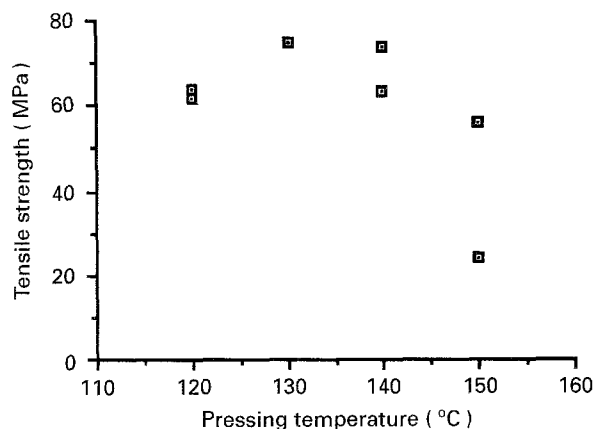


Figure 14 The influence of the pressing temperature on the tensile strength in the CSC-PAM system.

size, probably because water vapour pressure creates bubbles and cracks in the matrix (Fig. 13). The overall effect is a maximum, then a sharp decrease of the tensile strength (Fig. 14).

#### 4. Conclusion

MDF cements show very high fracture strengths due to both a high stress intensity factor, and a small critical defect size.

An investigation of PVA-aluminate ion films allowed us to discuss the origin of the high  $K_{IC}$ . Ionic cross-linking, although present, is probably not the main toughening mechanism occurring in these cements, because the tensile strength of the films was seen to decrease with the addition of aluminate ions. The high critical stress intensity factor was ascribed to the composite structure of the cement, which is observed at different scales: 15  $\mu\text{m}$  (cements grains) and 20 nm (hydrated products). Bridging effects were also shown to have an influence on the fracture work.

On the other hand, the critical defect size is also a very important parameter affecting the mechanical properties. It was shown that changing the processing variables (molecular weight, or pressing temperature, for examples) may have an influence on both  $K_{IC}$  and  $a_c$ , leading to complicated evolutions of the tensile strength.

#### Acknowledgements

L. Salin, N. Riche and C. Dupoisson are thanked for their technical support.

#### References

1. J. D. BIRCHALL, A. J. HOWARD, K. KENDALL and J. H. RAISTRICK, US Pat. 4410 366, 18 October 1983.
2. *Idem*, *Nature* **289** (1981) 388.
3. O. O. POPOOLA, W. M. KRIVEN and J. F. YOUNG, *J. Am. Ceram. Soc.* **74** (1991) 1928.
4. R. RODGER, S. A. BROOKS, W. SINCLAIR, G. W. GROVES and M. DOUBLE, *J. Mater. Sci.* **20** (1985) 2853.
5. P. P. RUSSELL, MSc thesis, University of Illinois at Urbana-Champaign (1991).

6. I. TITCHELL and R. W. DAVIDGE, *J. Mater. Sci. Lett.* **8** (1989) 629.
7. R. G. HILL, A. D. WILSON and C. P. WARRENS, *J. Mater. Sci.* **24** (1989) 363.
8. E. A. WASSON and J. W. NICHOLSON, *Clin. Mater.* **7** (1991) 289.
9. M. F. VALLAT, P. ZIEGLER, P. VONDRACEK and J. SCHULTZ, *J. Adhes.* **35** (1991) 95.
10. R. K. SCHULTZ and R. R. MYERS, *Macromolecules* **2** (1969) 281.
11. R. RAHBARI and J. FRANÇOIS, *Polymer* **33** (1992) 1449.
12. Y. W. MAI, *Mater. Forum* **11** (1988) 232.
13. R. C. SAKAI and R. C. BRADT, *Nippon, Seramikkusu Kyokai Gakujutsu Ronbunshi* **96** (1988) 801.
14. R. M. L. FOOTE and V. T. BUCHWALD, *Int. J. Fract.* **29** (1985) 125.
15. Y. W. MAI and M. LAWN, *J. Am. Ceram. Soc.* **70** (1987) 290.

*Received 8 March 1994  
and accepted 3 February 1995*